CHEMICAL ENGINEERING TRANSACTIONS Volume 17, 2009
Editor Sauro Pierucci
 ISBN 978-88-95608-01-3 ISSN 1974-9791
DOI: 10.3303/CET0917095

Single Bubble and Drop Motion Modeling

Giulia Bozzano and Mario Dente
Politecnico di Milano, CMIC Department
Piazza L. da Vinci, 32, 20131 Milano, Italy

A model for the prediction of the terminal relative velocity of single gas bubbles or drops, moving into a quiescent liquid phase, is presented. Also the effect of contamination is taken into account. It has been compared with a large set of experimental literature data covering a wide range of physical properties and particle sizes. The agreements are quite satisfactory and confirm the reliability of the model.

Introduction

The characterisation of bubbles or drops motion is essential for many gas-liquid and liquid-liquid operations, not only related to chemical processes but also, for instance, to metallurgy, biotechnology and oceanography. Even if in practical applications the overall motion regards swarms, the behavior of the single fluid particle can support a better knowledge of the overall. Modeling the single particle behavior can be considered a quite complex problem by itself, particularly if the purpose is to cover a wide range of properties. Some theories have been presented along the years, covering different fluid-dynamic regimes, shapes and, correspondingly, drag coefficients (Harmathy, 1960; Levich, 1962; Batchelor, 1970; Bhaga *et al.*, 1981; Karamanev, 1994, Nguyen, 1998; Kelbaliyev *et al*., 2007). Starting from the studies of Hadamard (1911) and Rybczynsky (1911) based on spherical shape fluid particles in completely viscous flow, many studies were performed taking into account different shapes and trying to deduce more or less empirical correlations for the drag coefficient. More detail on these studies is given in Bozzano and Dente (2001), where is proposed a solution for the prediction of shape and velocity of bubbles inside quiescent liquids. Here an extension to the case of drops is presented. The differences are mainly related to the viscosity of the fluid particle. Again the shape is estimated by minimizing the total energy associated to motion.

Shape of the Dispersed Particle and Drag Coefficient

The prevailing particle motion is assumed linear (secondary motions, i.e. helicoidal, zig-zag, oscillating etc. are neglected). The shape is assumed being the superposition of two oblate semi-spheroids (figure 1) having in common the larger semi-axis. Asymptotically this shape can degenerate towards a spherical-cap (b_2=0) or a sphere ($a= b_1= b_2$).

Please cite this article as: Bozzano G. and Dente M., (2009), Single bubble and drop motion modeling, Chemical Engineering Transactions, 17, 567-572 DOI: 10.3303/CET0917095

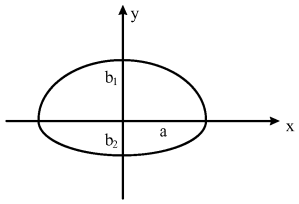

Fig. 1 – Basic shape of the fluid particle (a, b_1, b_2 = particle major and minor semi-axes)

Of course a fluid particle differs from that of a rigid body mainly for two aspects: the possibility of adapting its shape and the presence of internal recirculations. They deeply affects the resistance to the particle motion. In the steady state the forces balance gives:

$$\Delta\rho \cdot g \cdot V_p = \pi a^2 \frac{\rho_c U^2}{2} \cdot f \tag{1}$$

Therefore the terminal velocity (U) is deduced as a function of the drag coefficient (C_D):

$$U = \left(\frac{4}{3} \frac{\Delta\rho \cdot g \cdot D_0}{\rho_c C_D} \right)^{1/2} \qquad \text{where } C_D = \left(\frac{2a}{D_0} \right)^2 \cdot f \tag{2}$$

The key variable is the drag coefficient C_D. It shows a simple dependence on the friction factor "f" and on the deformation of the particle. The particle assumes during its motion the shape that minimizes its total energy. Substantially the energies mainly involved (interfacial, potential and kinetic, already described in Bozzano and Dente, 2001) reflect the influence of interfacial tension, density difference, viscosity and velocity on the particle shape. The presence of contaminants or hydrates at the interface affects its rigidity and the internal recirculation. The mapping of the total energy as a function of the particle geometrical properties allows to deduce "Def" By the proper regression of the minimization procedure results, an explicit expression for "Def" has been deduced:

$$Def = \left(\frac{2a}{D_0} \right)^2 = \frac{10 \cdot \left(1 + 1.3 \cdot Mo^{1/6}\right) + 3.1 \cdot Eo}{10 \cdot \left(1 + 1.3 \cdot Mo^{1/6}\right) + Eo} \tag{3}$$

The friction factor can be obtained by combination of asymptotic behaviors, viscous flow: f_{visc} , and Newton's-law flow: f_∞: $f(Re, Eo) = f_{visc}(Re, Mo) + f_\infty(Eo, Mo)$. For spherical shape particles (Def = 1), and low Re values, the drag coefficient has been evaluated (Batchelor 1970) as:

$$C_D = f_{visc} = \frac{48}{Re} \tag{4}$$

A correction was proposed by Moore (1963), taking into account the dissipation in the

boundary layer around the particle and in the wake:

$$f_{visc} = \frac{48}{Re}\left(1 - \frac{2.2}{Re^{1/2}}\right) \tag{5}$$

In expression 5) the negative factor can give place to problems at low Re values. A more satisfactory expression is here proposed:

$$f_{visc} = \frac{48}{Re} \cdot \frac{\sqrt{1 + 0.25\,Re}}{\sqrt{1 + 0.25\,Re} + 1} \tag{6}$$

The final expression of f_{visc} is:

$$f_{visc} = \frac{48}{Re} \cdot \frac{\sqrt{1 + 0.25\,Re}}{\sqrt{1 + 0.25\,Re} + 1} \cdot \frac{3/2 + \mu_c/\mu_d}{1 + \mu_c/\mu_d} \cdot \frac{1 + 12 \cdot Mo^{1/3}}{1 + 36 \cdot Mo^{1/3}} \tag{7}$$

(the viscosity ratio accounts for the effect of internal recirculation: Batchelor, 1970). The last factor in expression 7) is a combination of asymptotic behaviors reducing the factor "48" to "16" for high Mo and reflecting the typical behavior in high viscosity medium. The drag coefficient ($C_D\big|_\infty$) for sufficiently high Reynolds numbers (at least 10^4), becomes a constant corresponding to about 3 because of the large deformation (spherical cap shape). The asymptotic friction factor is also deduced as function of Eo and Mo:

$$f_\infty = \frac{C_D\big|_\infty}{DEF\big|_\infty} = 0.9\frac{Eo^{3/2}}{1.4 \cdot \left(1 + 30Mo^{1/6}\right) + Eo^{3/2}} \tag{8}$$

Then the combined expression of the friction factor becomes (with c,d = indexes for continuous and dispersed phase):

$$f = \frac{48}{Re} \cdot \frac{\sqrt{1 + 0.25Re}}{\sqrt{1 + 0.25Re} + 1} \cdot \frac{3/2 + \mu_c/\mu_d}{1 + \mu_c/\mu_d} \cdot \frac{1 + 12 \cdot Mo^{1/3}}{1 + 36 \cdot Mo^{1/3}} + 0.9\frac{Eo^{3/2}}{1.4 \cdot \left(1 + 30Mo^{1/6}\right) + Eo^{3/2}} \tag{9}$$

Internal recirculations of drops are less intensive than inside bubbles forcing the detachment of the boundary layer on a larger surface. Therefore, *for drop motion,* the friction factor is modified in:

$$\begin{aligned} f_\infty < 0.45 \quad & f = \frac{48}{Re} \cdot \frac{\sqrt{1 + 0.25Re}}{\sqrt{1 + 0.25Re} + 1} \cdot \frac{3/2 + \mu_c/\mu_d}{1 + \mu_c/\mu_d} \cdot \frac{1 + 12 \cdot Mo^{1/3}}{1 + 36 \cdot Mo^{1/3}} + 0.45 \\ f_\infty \geq 0.45 \quad & f = \frac{48}{Re} \cdot \frac{\sqrt{1 + 0.25Re}}{\sqrt{1 + 0.25Re} + 1} \cdot \frac{3/2 + \mu_c/\mu_d}{1 + \mu_c/\mu_d} \cdot \frac{1 + 12 \cdot Mo^{1/3}}{1 + 36 \cdot Mo^{1/3}} + 0.9\frac{Eo^{3/2}}{1.4 \cdot \left(1 + 30Mo^{1/6}\right) + Eo^{3/2}} \end{aligned} \tag{10}$$

Results and Comparisons

The figures compare model results (lines), and experimental data (points). They are a representative sample of the total results. Figgs 2-7 refer to air-liquid systems (2 to 6, experiment from Peebles and Garber (1953), Fig. 7 those of Haberman and Morton (1956)), while figs 8-13 show liquid-liquid behavior. The properties of liquids are reported in Table 1.

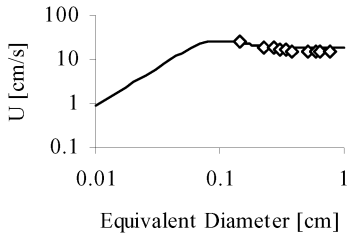

Fig. 2: Air bubbles in ethylacetate

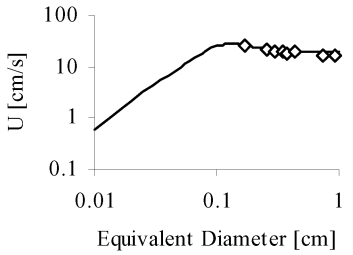

Fig. 3: Air bubbles in pyridine

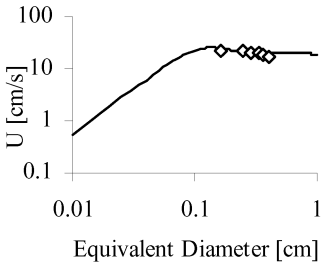

Fig. 4: Air bubbles in 70% Acetic acid –water solution (AAW)

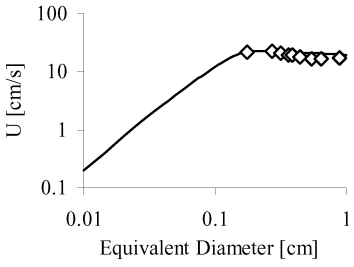

Fig.5: Air bubbles in Aniline

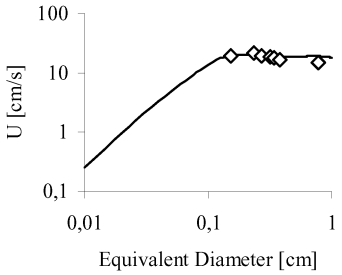

Fig.6: Air bubbles in Isopropyl Alcohol (IPA)

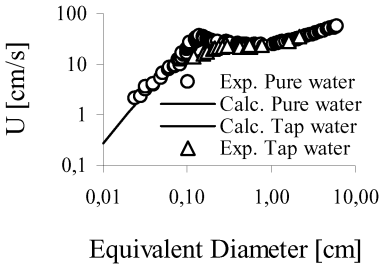

Fig.7: Air bubbles in purified and tap water

Table 1: properties of air-liquid systems

	AAW	Aniline	IPA	Ethylacetate	Pyridine
ρ_c (g/cm^3)	1.0684	1.02	0.793	0.894	0.987
μ_c (g/cm/s)	0.0104	0.0293	0.0178	0.0047	0.0085
σ (g/s^2)	34.3	41.7	20.7	22.6	36.6

Figure 8 reports some interesting data related to the fall of liquid CO_2 drops in the deep Ocean. The experiments (data from Ozaki *et al.*(2001)) where performed at 200 atm and 5°C in order to study the possible CO_2 ocean sequestration by moving ships. Figs 9-13 compare the model with the data of Shengen Hu and Kintner (1955) on different organic liquids. Table 2 refers to the properties of the analyzed systems.

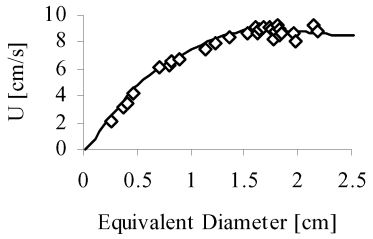

Fig.8: CO_2 drops in deep sea (SW-CO_2)

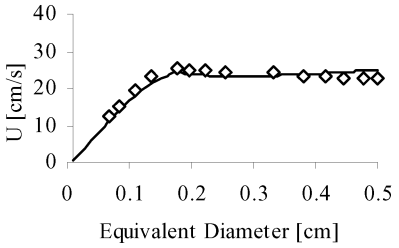

Fig. 9: Water-tetrabromoethane (WT)

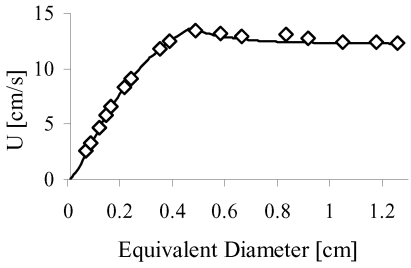

Fig. 10: Water-nitrobenzene (WN).

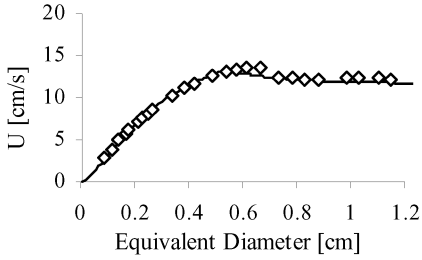

Fig. 11: Water-O-nitrotoluene (WON)

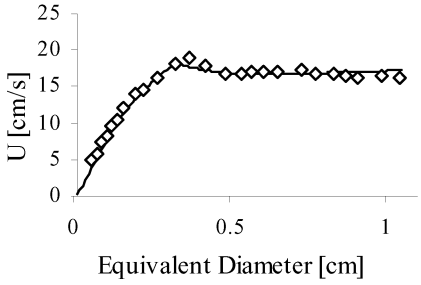

Fig. 12: Water-bromobenzene (WBB)

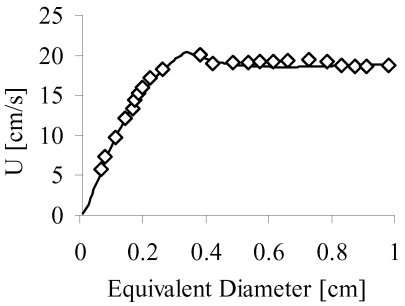

Fig. 13: Water-tetrachloroethylene (WTCl)

Table 2: properties of liquid-liquid systems

	SW-CO_2	WT	WN	WON	WBB	WTCl
ρ_d (g/cm^3)	1.050	2.9474	1.1947	1.1576	1.4881	1.6143
ρ_c (g/cm^3)	1.024	0.9973	0.9972	0.997	0.9971	0.9970
μ_c (g/cm/s)	0.0158	0.008968	0.008835	0.008996	0.008953	0.008946
μ_d (g/cm/s)	0.00125	0.092888	0.017379	0.02036	0.010719	0.008903
σ (g/s^2)	42.0	35.9	28.9	31.3	36.3	44.4

Conclusions

All the comparisons show the reliability of the proposed model in a wide range of conditions (both for particle size and physical properties). The new approach allows a unified model for the description of bubbles or drops motion into quiescent liquid.

Nomenclature

D_0 = diameter of the equivalent spherical fluid particle (m)
g = acceleration due to gravity (m/s^2)
ρ, $\Delta\rho$ = density and density difference (kg/m^3), σ = interfacial tension (N/m), μ = viscosity (kg/(ms))

Reynolds, Eötvös and Morton numbers: $\mathrm{Re} = \frac{\rho_c D_0 U}{\mu_c}$ $\mathrm{Eo} = \frac{\Delta\rho\, g\, D_0^2}{\sigma}$, $\mathrm{Mo} = \frac{\Delta\rho \cdot g\, \mu_c^4}{\rho_c^2 \sigma^3}$

References

Batchelor, G.K., 1970, An Introduction to Fluid-dynamics. Cambridge University Press

Bhaga D. and Weber M.E., 1981, Bubbles in viscous liquids: shapes, wakes and velocities, Journal of fluid Mechanics, 105, 61-85

Bozzano G. and Dente M. , 2001, Shape and terminal velocity of single bubble motion: a novel approach, Comp. & Chem. Engng., 25, 571-576

Bryn, T., 1949, David Taylor Model Basin Transl., Rep. No 132

Calderbank, P. H., Johnson, D. S. L. and Loudon, J., 1970, Mechanics and mass transfer of single bubbles in free rise through some newtonian and non-newtonian liquids, Chem. Eng. Sci., 25, 235-256

Davies R.M. and Taylor F.R.S. Sir Geoffey, 1950, Proceedings of the Royal Society, A200, 375-390

Haberman, W. L. and Morton, R. K., 1956, Soc. Civil Eng. Trans., 121, 227-251

Hadamard, J., 1911, Movement permanent lent d'une sphere liquide et visqueuse. dans un liquide visqueux, Comptes Rendus Hebdomadaires des Seances de l' Academie des Sciences, 152, 1735-1743

Harmathy T.Z., 1960, Velocity of large drops and bubbles in media of infinite or restricted extent, A.I.Ch.E. Journal, 6, No.2, June, 281-288

Karamanev D.G. , 1994, Rise of Gas Bubbles in Quiescent Liquids, A.I.Ch.E. Journal, 40, no. 8, August, 1418- 1421

Levich, V.G. , 1962, Physico-chemical hydrodynamics, New York, Prentice-Hall

Moore, D.W. , 1963, The boundary layer on a spherical gas bubble, J. Fluid Mech., 16, 161-176

Ozaki M. Minamiura J., Kitajima Y., Mizokami S., Takeuchi K. and Hatakenaka K., 2001, CO_2 ocean sequestration by moving ships, J. Mar. Sci Technol, 6, 51–58

Peebles, F. N., Garber, H. J., 1953, Studies on the motion of gas bubbles and liquids, Chem. Eng. Progr., 49, 88-97

Rybczynski, 1911, Über die fortschreitende Bewegung einer flüssigen Kugel in einem sachen Medium, Bull. Intern. Acad. Sci. Cracovie (Ser. A) 1, 40-46.

Shengen Hu, Kintner R.C., 1955, The fall of single liquid drops through water, A.I.Ch.E. Journal, 1, No.1, March, 42-48